Analytical Methods

Accepted Manuscript

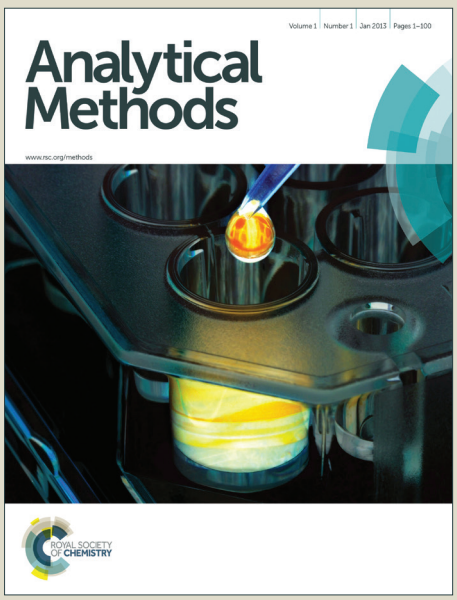

This is an *Accepted Manuscript*, which has been through the Royal Society of Chemistry peer review process and has been accepted for publication.

Accepted Manuscripts are published online shortly after acceptance, before technical editing, formatting and proof reading. Using this free service, authors can make their results available to the community, in citable form, before we publish the edited article. We will replace this *Accepted Manuscript* with the edited and formatted *Advance Article* as soon as it is available.

You can find more information about *Accepted Manuscripts* in the Information for Authors.

ROYAL SOCIETY OF CHEMISTRY

www.rsc.org/methods

Characterization of Peucedani Radix extract-derived angular-type pyranocoumarins in rats using ultra high performance liquid chromatography coupled with hybrid triple quadrupole-linear ion trap mass spectrometry

Yuelin Song [a,b#], Wanghui Jing [a#], Pengfei Tu [b,c], Yi-Tao Wang [a]*

[a] State Key Laboratory of Quality Research in Chinese Medicine, Institute of Chinese Medical Sciences, University of Macau, Macao SAR, 999078, P.R. China;

[b] Modern Research Center for Traditional Chinese Medicine, Beijing University of Chinese Medicine, Beijing, 100029, P. R. China;

[c] State Key Laboratory of Natural and Biomimetic Drugs, School of Pharmaceutical Sciences, Peking University, Beijing, 100191, P.R. China.

*Correspondence author:

Prof. Yi-Tao Wang

State Key Laboratory of Quality Research in Chinese Medicine, Institute of Chinese Medical Sciences, University of Macau, Macao SAR, China

E-mail: ytwang@umac.mo; Tel: +853 8397 4691; Fax: +853 2884 1358.

[#]: these two authors contributed equally to this paper.

Abstract

Active components of herbal medicine usually become trace in the body owing to absorption/distribution barrier and/or biotransformation hurdle. The present study aims to detect and identify angular-type pyranocoumarins (APs) in biological samples (plasma, urine and feces) obtained from rats after oral intake of Peucedani Radix extract (PRE) adopting ultra high performance liquid chromatography-tandem mass spectrometry. Initially, 11 reference compounds were used to identify their prototypes. And then, a prediction for the *in vivo* compounds was performed on the basis of chemical profiling for PRE and metabolic pathway characterization for APs in our previous reports, and the prediction was subsequently transferred to give birth to a predictive multiple ion monitoring-information dependent acquiring-enhanced product ion (pMIM-IDA-EPI) procedure. Besides 10, 8, 8 pyranocoumarins were unambiguously identified in plasma, urine and fecal samples with the help of authentic compounds, respectively, chemical structures of another 21 ones (8 prototypes and 13 metabolites) in plasma, 10 ones (6 prototypes and 4 metabolites) in urine and 8 (4 prototypes and 4 metabolites) in feces were tentatively assigned based on their mass spectral profiles. Collectively, the method adopting pMIM-IDA-EPI mode was demonstrated to be reliable and can be introduced as a rational implement for rapid characterization of herbal medicine-derived components in biological samples.

Keywords: predictive multiple ion monitoring; angular-type pyranocoumarins; metabolites; Peucedani Radix; hybrid triple quadrupole-linear ion trap mass spectrometry

1. Introduction

Chemical drugs are more and more challenged by side effects and multidrug resistance [1-4]. On the other side, as multi-component and multi-target agents, herbal medicines exert a holistic therapeutic action [5], thus playing an increasing crucial role in the treatment of chronic diseases today. However, the characterization of the active material basis that plays a therapeutic role cannot be easily achieved. One feasible way is to identify the *in vivo* components since only the exposed chemicals could play the therapeutic role in most cases [6]. However, herbal medicine usually contains numerous components in minor amounts and those naturally occurring in high amounts in the original herb are likely to become trace in the body due to absorption/distribution barrier and/or biotransformation hurdle. As a consequence, more sensitive and selective methods should be introduced for better understanding of the pharmacological basis when herbal medicine-treated biological samples were analyzed.

Angular-type pyranocoumarins (APs), which are also known as khellactone derivatives, such as (±)-praeruptorin A (PA), (±)-praeruptorin B (PB), and (+)-praeruptorin E (*d*PE), are widely documented as the main chemical constituents in Peucedani Radix (Chinese name: Qian-hu) [7,8], which has been utilized for the treatment of cough with thick sputum and dyspnea, upper respiratory infections, and nonproductive cough for centuries in traditional Chinese medical practices [9-10]. APs have been widely demonstrated that they can act as anti-HIV agents [11] and P-glycoprotein modulators [12], in particular, hypotensor candidates, typically through acting as calcium channel blocker and potassium channel opener [13,14].

Hybrid triple quadrupole-linear ion trap mass spectrometer (Q-trap-MS) owns tandem mass spectrometry (MS/MS) functions including neutral loss (NL) scan, precursor ion (PI) scan, multiple reaction monitoring (MRM) of traditional triple quadrupole mass spectrometer (QqQ-MS) and enhanced product ion (EPI) scan, enhanced resolution (ER) scan and enhanced mass spectrum (EMS) scan of the linear ion trap instruments [15-19]. Information-dependent acquisition (IDA) is a procedure that

could combine two or more different measurement modes in a sequential for a single LC-MS/MS run [20]. Multiple ion monitoring (MIM) mode, a special MRM mode with fixed collision energy (CE) of 5 eV in the q2 cell, offers comparable sensitivity to a vast number of analytes, while reference compounds are not required for the optimization of ion transition mass parameters [21]. Given that most drug-related components existed as prototypes as well as their metabolites *in vivo*, a predictive MS/MS mode based on the results of original herb chemical profiling and potential biotransformation pathways of analytes should be more suitable for rapid screening and identification of herb medicine-related trace components in biological samples. In our previous studies, predictive MIM-IDA-EPI (pMIM-IDA-EPI) and predictive MRM-IDA-EPI (pMRM-IDA-EPI) modes were introduced to rapidly and rationally characterize the metabolic profiles of carnosic acid and (±)-praeruptorin A, respectively [22,23]. However, the ion transitions for pMIM-IDA-EPI mode were quite less than that for the latter one, and also it is unnecessary to optimize CE value for each ion transition. Therefore, pMIM-IDA-EPI mode was adopted to characterize the Peucedani Radix extract (PRE)-derived components in rat in current study.

The fragmentation patterns of APs were reported previously [24]: neutral loss occurs at C-4′ position initially to form a stable intermediate ion; the intermediate ion will further lose another neutral molecule from the C-3′ position to produce a fragment ion at *m/z* 227 or remove a acyl group to yield a product ion at *m/z* 245; the single acyl substituent would be cleaved whether it located at C-3′ or C-4′ position, when C-4′ or C-3′ existed in the keto form. With the assistance of these features, chemical profiling of PRE was achieved using LC-MS/MS [24]. In addition, the reported metabolic pathways of APs include oxidation, hydrolysis, intra-molecular acyl migration and glucuronidation [22,25-29].

To understand the effective material basis of this herbal drug, in the present study, a practical method employed ultra high performance liquid chromatography (UHPLC) coupled with Q-trap-MS was proposed to characterize the herb-related APs in biological samples after oral administration of PRE. The APs' prototypes and their

metabolites appearing in biological samples were characterized using the pMIM-IDA-EPI mode. The findings obtained are expected to be meaningful for revealing the actually active forms being responsible for the benefits of Peucedani Radix in biological samples.

2. Experimental

2.1 Chemicals

APs, including *cis*-khellactone (CKL), *cis*-4′-angeloylkhellactone (CAK-4), *trans*-4′-angeloylkhellactone (TAK-4), *trans*-3′-angeloylkhellactone (TAK-3), *cis*-3′-acetyl-4′-angeloylkhellactone (AAK), praeruptorin A (PA), *cis*-3′-isovaleryl-4′-acetylkhellactone (IAK), praeruptorin B (PB), *cis*-3′-angeloyl-4′-senecioylkhellactone (ASK), praeruptorin E (PE) and *cis*-3′,4′-diisovalerylkhellactone (DIK) were isolated from Peucedani Radix in our group previously [24]. All the chemical structures and purities (Fig. 1) were identified using NMR and LC-MS/MS analyses.

Formic acid and acetonitrile were of HPLC grade and purchased from Merck (Darmstadt. Germany). Deionized water was prepared in house using Milli-Q plus water purification system (Millipore, Bedford, MA, USA). All other chemicals were of analytical grade and obtained commercially.

2.2 Preparation of samples

2.2.1 Reference samples

All reference compounds were dissolved in 50% aqueous ACN respectively and then filtered through 0.45 μm nylon membrane (Jinteng Experiment Equipment Co. Ltd., Tianjin, China) to obtain reference samples. The reference compounds mixture was prepared by mixing all the reference samples and stored in a refrigerator (4°C) until use.

PRE was prepared in our group previously [26]. An aliquot (10 mg) of the crude extract was dissolved in 1 mL 50% aqueous ACN and then ultrasonic water bathing for 10 min. The obtained solution was centrifuged at 15 000×*g* for 10 min and the

supernatant was filtered through 0.45 μm nylon membrane (Jinteng Experiment Equipment Co., Ltd.) to afford the extract sample.

2.2.2 Preparation of biological samples

The whole *in vivo* protocol was approved by the Animal Ethics Committees of University of Macau. Male Sprague-Dawley rats (220 ± 15 g) were purchased from Guangdong Medical Laboratory Animals Center (Guangzhou, China) and acclimated in laboratory for one week prior to the experiments. Animals were randomly divided into the vehicle group (n = 3) and the PRE group (n = 3), and each rat was housed in separate metabolic cage with free access to standard diet and water at a temperature of 23 ± 1°C with a 12 h light/dark cycle and relative humidity of 50%. Before the oral treatment, a cannula for blood sampling was implanted at the jugular vein and rats were fasted for 12 h, yet water *ad libitum*.

50% aqueous 1,2-propylene glycol solution of PRE was orally administered at a dose of 1000 mg/kg to rats from PRE group, while each vehicle group rat received equal volume of 50% aqueous 1,2-propylene glycol solution. A 250 μL aliquot of blood samples were collected at 30 and 60 min from the implanted cannula after oral administration for each rat, and then centrifuged at 3 000×g at 4°C for 10 min to yield plasma samples. An aliquot (100 μL) of plasma was mixed with equal volume of acetonitrile, vortex-mixed and centrifuged at 15 000×g, 4°C for 10 min to remove the protein. Urinary sample over 0-24 h of each rat was collected and pooled within group, and then mixed with equal volume of acetonitrile for desalting. The mixture was vortexed and centrifuged, and then the supernatant was filtered through 0.45 μm membrane and subjected for the LC-UV-MS/MS analysis. Pooled fecal sample that collected over 0-24 h from either group was extracted with acetonitrile at 10 mL per gram fecal sample for 30 min using ultrasonic water bath and then filtered through 0.45 μm membrane before analysis.

2.3 LC-UV-MS/MS analysis

LC-UV domain was an Agilent series 1200SL (Agilent Technologies, Palo Alto, CA, USA) liquid chromatographic system, equipped with a vacuum degasser, a binary

pump, an auto-sampler, and a diode array detector (DAD). Mass spectrometry was completed on an API4000 Q-trap® mass spectrometer (ABSciex, Foster City, CA, USA) equipped with a Turbo V™ Ion Source. Analyst Software package (Version 1.5, ABSciex) was used to control the whole system and for data acquisition and processing.

The chromatographic separation was achieved on a ZORBAX SB-C_{18} column (100 × 2.1 mm i.d., particle size 1.8 μm, Agilent). The mobile phase consisted of 0.1% aqueous formic acid (A) and acetonitrile containing 0.1% formic acid (B), and a gradient elution was adopted as follows: 0-65 min, 23%-75%B; flow rate 0.22 $mL \cdot min^{-1}$. The duration between different injections was set as 10 min for system equilibration. The column temperature was maintained at 35°C. The injection volume was 2 μL. UV absorbance over 190-400 nm was recorded.

Positive ion optics was tuned using standard polypropylene glycol (PPG) dilution solvent. Nitrogen was used as the nebulizer, heater, curtain and collision gas. Ion source parameters were optimized as follows: nebulizer (GS1), heater (GS2) and curtain gas flow rates 40, 40, 15 units, respectively; ionspray needle voltage, 5 500 V; heater gas temperature, 400°C; CAD gas, high level.

The mass parameters of all the 11 authentic compounds were optimized using syringe pump (Harvard HA22I, Instech Laboratories, Inc., Plymouth Meeting, PA) continuous infusion analysis. MRM mode was chosen for monitoring reference compounds in biological samples, while the extract sample and reference compound mixture were also analyzed in parallel to verify the identification. For each reference compound, two ion pairs were adopted and the optimal DP and CE values for each precursor-product ion transition were summarized in Table 1.

pMIM-IDA-EPI mode was adopted to analyze the biological samples. Extract sample and reference compound mixture were also tested in parallel to assist the identification of components *in vivo*. As mentioned above, oxidation, hydrolysis and acyl migration were the main metabolic types of those pyranocoumarins. Therefore, in the present study these reaction types as well as sulfation and glucuronidation were

introduced to predict potential metabolites. In addition, our previous studies revealed the sodium adduct ions as the most abundant quasi-molecular ion for most parent pyranocoumarins detected in the herbal extract and the metabolites of some pyranocoumarins formed *in vitro* [24-29]. The sodium adduct ion was thereby adopted as the precursor ion for parent pyranocoumarins and their metabolites *in vivo* with exception of khellactone, of which both sodium adduct and protonated ions were used as precursor ions in both. For the survey scan, the MIM mode employed a minimal CE (5 eV) in collision cell (q2) so that target ions isolated in the first quadrupole cell passed through q2 cell with minimal fragmentation, and then the same precursor ions, instead of fragment ions, were trapped in the LIT cell to generate product ions by dependent EPI experiments. For the three separate EPI scans, the threshold of ion intensity was set as 500 cps and the CE was set at 30 eV with a collision energy spread (CES) of 15 eV. Dynamic fill time (DFT) function was applied to ensure that the linear ion trap is not overfilled. The total cycle time was approximate 2.04 s.

2.4. Lower limits of detection (LLODs) for pMIM and MRM modes

The reference compound mixture was diluted to a series of appropriate concentrations, and an aliquot of each diluted solution was injected into LC-UV-MS/MS system for MRM and pMIM-IDA-EPI analyses. The lower limits of detection (LLODs) were determined under either mode at a signal-to-noise ratio (S/N) of about 3.

3. Results and discussion

3.1 Lower limits of detection (LLODs) for pMIM and MRM modes

By serial dilution of the mixed reference solution, all the LLODs of CKL, CAK-4, TAK-4, TAK-3, AAK, PA, IAK, ASK, PB, PE and DIK were determined less than 1 $ng \cdot mL^{-1}$ under the MRM mode (Fig. S1). At the meanwhile, all the LLODs of these reference compounds under MIM conditions were determined less than 2 $ng \cdot mL^{-1}$ (Fig. S2). Therefore, MIM mode showed comparable and satisfactory sensitivity to MRM mode for qualitative analysis of APs in biological samples.

3.2 Procedure for the identification of APs in PRE-treated biological samples

Since the extract-related components may exist *in vivo* as both forms of prototype and metabolite(s), and generally most are in minor amounts, the following steps were adopted to identify APs in PRE-treated biological samples.

First, reference compounds were used to confirm those components existed in biological samples as parent compounds using a couple of precursor-product ion transitions with optimum collision energy in MRM mode (Table 1). The retention time of each reference compound and the ratio of ion transitions were also adopted as the evidences for characterization of the identities.

Second, the chromatograms that obtained using pMIM-IDA-EPI of samples from the PRE group and the vehicle group were carefully compared to confirm the additional peaks in treated samples. Those additional peaks that also existed in the chromatogram of extract sample at the corresponding retention times were regarded as herb originated components, while the other peaks were characterized as metabolites. And then, the MS^2 spectral values of those herbal originated APs were used to confirm the identification of prototype components *in vivo* by comparing with those data observed in herbal extract [24].

Third, the molecular weight of the metabolites which existed as additional peaks in treated samples yet absent in extract chromatogram, was fixed by the predefined sodium adduct ion. The product ions of these chemical components were obtained using the EPI scan triggered by the pMIM survey experiment and used to identify these metabolites on the basis of the fragmentation pathways proposed previously in combination with the prediction of metabolic types.

3.3 Characterization of APs in biological samples after PRE treatment

After oral administration of PRE to rats, 10 APs were unambiguously identified in plasma, while eight APs were observed in either urine or fecal samples using reference compounds (Table 1). Meanwhile, 8 APs prototypes were characterized without references compounds in plasma by comparison of the additional peaks in treated plasma with the extract sample, and 6 and 4 herbal originated components

were detected in urine and fecal samples, respectively. Moreover, 13, 4 and 4 APs metabolites were observed and tentatively assigned based on their mass spectral profiles in plasma, urine and feces from PRE group, respectively. The retention times, predefined metabolic types, mass spectroscopic data and identification were summarized in Table 2.

3.3.1 Characterization of APs' prototypes using MRM mode combined reference compounds

CKL was predefined by precursor-product ion transitions of 263>245 and 263>203 with retention time of 3.99 min in plasma, urine and feces (Table 1, Fig.2). In addition, the intensity ratio of these two ion transitions also supported that the component eluted at 3.99 min in biological samples was CKL. On the other side, CAK-4, TAK-4, TAK-3, PA, IAK, PB, ASK, PE and DIK were detected by their characteristic precursor-product ion transitions with optimal collision energies, the intensity ratios of ion transitions and retention times of 23.31 min, 24.55 min, 25.43 min, 36.30 min, 38.34 min, 45.20 min, 46.91 min, 49.24 min and 51.78 min, sequentially, in plasma, urine and feces of rats (Table 1, Fig. 2). However, AAK, which was observed as one of the main constituents in extract (Fig. 2A), were absent in plasma, urine and feces according to the MRM mode, indicating this compound was transferred into its metabolites absolutely or unabsorbed at all. The stability test of AAK was performed in rat plasma, revealing that crucial carboxylesterase(s)-catalyzed hydrolysis occurred for these components [30].

It's interesting to note that the ratio of CKL (263>203) *vs.* PA (409>227) in plasma, urine or feces was much higher than that in the extract, and the ratios of CKL *vs.* other known APs also ascended by comparison with extract samples and treated biological samples (Fig. 2). Thus, CKL might be the main drug-related component in rat after oral administration of PRE judging on basis of its peak area, which was consolidated by the findings obtained previously [31]. Moreover, the high concentrations of APs in fecal samples (Fig. 2) indicated crucial absorption barriers for APs.

3.3.2 Characterization of APs' prototypes using pMIM mode

The chemical profile of PRE was characterized in our group previously [24], and 42 APs were tentatively identified. In current study, compounds **1**, **6-8**, **11-13**, **17**, **19**, **22**, **33** and **35** in plasma, compounds **1**, **6**, **11**, **33** and **35** in urine and compounds **1**, **7**, **8**, **11**, **13** and **19** in feces were detected as prototypes using pMIM-IDA-EPI scan by comparing retention times, MS^1 and MS^2 spectral profiles with those in PRE (Table 2).

3.3.3 Identification of pyranocoumarin metabolites *in vivo*

The khellactone derivative observed in the herbal extract usually consists of the skeleton with two acyl groups at the C-3′ and C-4′ position. The metabolic stability results revealed that oxidation initiated for acyl groups at either C-3′ or C-4′ position, while hydrolysis only occurred for the ester groups at C-3′ and/or C-4′ positions [25,26]. Hydroxylation didn't occur at the coumarin-skeleton (C-3 to C-6 positions) of angular-type pyranocoumarins [29]. As described previously [24], acetyloxy, 2-isobutyroyloxy, angeloyloxy, isovaleryloxy, seneciolyloxy, tigloyloxy, 2-methylbutyryloxy and isovaleryloxy groups were observed most frequently for the APs from the Peucedani Radix, therefore hydrolyzed products generated by the loss of these acyl substituents might exist *in vivo*. Additionally, hydroxylation and hydration could occur for those groups with ethylenic bond, such as angeloyloxy, seneciolyloxy and tigloyloxy groups, while hydroxylation could be observed for isovaleryloxy, 2-isobutyroyloxy and 2-methylbutyryloxy groups. Moreover, glucuronidation and sulfation might occur when dissociative hydroxyl groups present in chemical components, indicating that the glucuronidated and/or sulfated metabolites of khellactone might exist *in vivo*. Therefore, the potential MIM transitions were proposed and summarized in Table 2.

Based on the presupposed MIM transitions, nine oxidated metabolites were detected in plasma, while two glucuronidated products were observed in the PRE-treated urine and feces (Table 2).

Precursor ion of metabolite at *m/z* 261, which was predefined as sodium adduct ion of hydrolyzed product of 3′-keto-3′,4′-dihydroseselin or

4′-keto-3′,4′-dihydroseselin derivates, such as compounds **22**, **24**, **27** and **28** [24], was observed at 4.04 and 4.14 min. The MS^2 spectra of these quasi-molecular ions showed the diagnostic cleavage of a water molecule (18 Da). As a consequence, these two metabolites were tentatively identified as 3′-keto-3′,4′-dihydroseselin and 4′-keto-3′,4′-dihydroseselin (Table 2). However, the elution order of these metabolites couldn't be determined due to the unavailability of these two regio-isomers.

Precursor ion of metabolite at *m/z* 383, which was predefined as sodium adduct ion of mono-oxidated product of CAK-4, TAK-4, TAK-3, compound **18** or **24** (*m/z* 367 $[M+Na]^+$), was eluted at 17.37 min. The MS^2 spectrum of this quasi-molecular ion showed the identical product ions of *m/z* 267 and 245 as CAK-4 and TAK-4, suggesting the neutral loss of HOC_4H_6COOH (116 Da) group and HOC_4H_6COONa (138 Da) group from the C-4′ position, respectively. Hence, this metabolite was identified as the mono-oxidated product of CAK-4 or TAK-4 according to the fragmental behaviors proposed before [24], and the oxidation occurred at the acyl substituent (Table 2).

Precursor ion of *m/z* 385 was presupposed as the sodium adduct ion of mono-oxidated products for compound **13**, **19** or **21** [24]. In the MS^2 spectra of this precursor ion, identical product ions at *m/z* 267 and 245 as compound **19** [24] were observed, suggesting the neutral losses of a $C_4H_8OHCOOH$ (118 Da) and $C_4H_8OHCOONa$ (140 Da) group, respectively. Thus, there was a mono-oxidated isovaleryloxy or mono-oxidated 2-methylbutyryl group substituted at the C-4′ position for these metabolites. Above all, the metabolites eluted at 12.10 min and 12.97 min in plasma were characterized as mono-oxidation of compound **19** at the isovaleryloxy moiety.

The precursor ion at *m/z* 401 was observed at the retention time of 9.01 min and defined as the sodium adduct ion of the di-oxidated metabolite of compound **13**,**19** or **21** [24]. The predominant product ions were exhibited at *m/z* 267 and 245, indicating the cleavage of a $C_4H_7(OH)_2COOH$ (134 Da) and $C_4H_8OHCOONa$ (156 Da) group from C-4′ position, respectively. Identical with the precursor ion at *m/z* 385, the metabolite

was identified as the di-oxidated product of compound **19** (Table 2), and the oxidation metabolism occurred at the isovaleryloxy substituent.

Five mono-oxidated product of PA was detected *in vitro* when PA was incubated with liver microsomal proteins [26]. Precursor ion at *m/z* 425, defined as the sodiated molecular ion of PA mono-oxidated products, was observed in plasma at the retention times of 17.58 min, 25.34 min and 26.15 min, and eluted at 42.89 and 31.36 min in either urine or feces (Table 2). In comparison of retention times and mass spectra profiles, precursor ion of *m/z* 425 eluted at 17.58 min, 26.15 min and 42.89 min also existed in herbal extract as compounds **11**, **17** and **33** [24], respectively. In the other hand, the MS^2 spectra of *m/z* 425 at 25.34 min and 31.36 min yielded characteristic product ions at *m/z* 365, suggesting the cleavage of an acetyl acid (60 Da), and the product ions at *m/z* 245 and 227 were also identical with those of PA. Therefore, the two metabolites, which were detected at 25.34 min and 31.36 min, were confirmed as the mono-oxidated products of PA, and the oxidation metabolism occurred for the angelyloxy group at C-3′ position.

Sodium adduct ion of *m/z* 427 was responsible for the detection of the mono-oxidation of IAK in pMIM survey scan and two metabolites were observed at 18.37 min and 19.75 min. MS^2 spectra of *m/z* 427 exhibited predominant product ion at *m/z* 367, suggesting the neutral loss of an acetyl acid moiety (60 Da) from the C-4′ position, which was the same as IAK. In addition, the presence of product ions at *m/z* 245 and 227 indicated the subsequent cleavage of a $C_4H_6OHCONa$ (122 Da) and a $C_4H_8OHCOONa$ (140 Da) group from C-3′ position, respectively. Consequently, both of them were identified as mono-oxidated products of IAK at C-3′ position (Table 2).

Two glucuronidated products of khellactone were also observed in biological samples. Precursor ions at *m/z* 439 (the same as the sodium adduct ion of compound **35** [24]) and *m/z* 461 were predefined as the protonated and sodium adduct ions of the glucuronidated metabolite of khellactone. Two potential metabolites were successively eluted at 1.90 min and 2.13 min. The neutral loss of a glucuronic acid (176 Da) to yielded characteristic ions at *m/z* 245 was observed in MS^2 spectra of both.

Therefore, the two compounds were characterized as glucuronidated metabolites of khellactone, and the glucuronidation could occur at either C-3′ or C-4′ position.

As mentioned in the metabolic profiling of *d*PB and *d*PE, mono-oxidation products of *d*PB and *d*PE were detected in rat liver microsomes *in vitro* [25]. Precursor ion at *m/z* 465, the sodiated molecular ion of PB mono-oxidation product, eluted at 38.23 min, while the mono-oxidation product (sodiated ion at *m/z* 467) of *d*PE was detected at 31.26 min. Further, the product ions at *m/z* 365 and 367 in the MS^2 spectra were observed for the precursor ions at *m/z* 465 and 467, respectively, both of which indicated the neutral loss of a C_4H_7COOH group from their corresponding precursor ions, while the product ions of *m/z* 245 and 227 revealed the further cleavages from C-3′ positions. Therefore, the metabolites eluted at 38.23 and 31.26 min were characterized as the mono-oxidated metabolites at C-3′ acyl group of PB and *d*PE, respectively.

Precursor ion at *m/z* 485, which was predefined to search the di-oxidated metabolite of DIK, was eluted at 19.78 min (Table 2). The product ions at *m/z* 367 indicated the neutral loss of a $C_4H_8OHCOOH$ (118 Da) group from the predefined precursor ion, and product ions at *m/z* 245 and 227 were generated by the further cleavage of $C_4H_6OHCONa$ (122 Da) and $C_4H_8OHCOONa$ (144 Da), respectively. Therefore, this metabolite was identified as di-oxidated product of DIK and oxidation metabolism occurred at both C-3′ and C-4′ positions of DIK.

Precursor ion of *m/z* 499, which was defined as mono-oxidation of compound **12**[24] in MIM survey scan, was eluted at 15.73 min in plasma. The major product ions at *m/z* 383 and 227 were yielded in MS^2 spectrum, indicating the neutral losses of a $C_4H_8OHCOOH$ (116 Da) group and a $C_4H_7(OH)_2COONa$ (156 Da) group, sequentially. Therefore, this peak was identified as mono-oxidation product of compound **12** at C-4′ position (Table 2).

The metabolism of several APs, such as *d*PA, *l*PA, *d*PB, *d*PE and DCK derivates [25,26,32-34], was characterized using the incubation system with liver microsomal proteins *in vitro*. All metabolisms were revealed occurring at the acyl groups linked to

C-3′ and C-4′ positions. Therefore, it is reasonable to believe that the biotransformation of pyranocoumarins *in vivo* only alert the acyl substituents instead of changing the khellacton skeleton. On the basis of speculation, the metabolites *in vivo* can be predicted. In addition, the software of PALLAS MetabolExpert (CompuDrug) [35] and METEOR MetabolicExpert (Lhasa) [36] were also introduced to predict the potential metabolites *in silico*, and the recommended metabolic types included hydrolysis and oxidation.

It is usually difficult to characterize the herb-related component exposed *in vivo* since: 1. herb extract is always regarded as a complex mixture of a large amount of chemical constituents; 2. the concentration of herb-related components is usually very low; 3. the compounds from extract frequently exist as parent and/or metabolite forms *in vivo*. It is reported that MIM-IDA-EPI had comparable sensitivity and selectivity to those of MRM-IDA-EPI and was more sensitive than EMS-IDA-EPI [37], thus MIM-IDA-EPI being selected in this study. In general, reference compounds were required to optimize the collision energy (CE) for each adopted ion transition under MRM mode, while MIM mode just use the quasi-molecular ion with the least CE as 5 eV without the employment of reference compounds. In addition, the information of product ions could be provided by the triggered EPI experiments. Therefore, the identities of chemical components in complex matrix could be characterized using the enough structural information provided by pMIM-IDA-EPI mode in the absence of reference compounds.

As the primary constituents of Peucedani Radix, APs underwent hydrolysis, oxidation and glucuronidation *in vivo*, and the metabolic pathways of those components were proposed in Fig. 3. However, intra-molecular acyl migration was observed as a major metabolic pathway for APs *in vitro*, yet undetectable *in vivo*, might owing that mono-esterificated products khellactone were observed in pairs in original herb, such as CAK-4 *vs*. compound **18**. As mentioned before, the concentration of CKL *in vivo* is quite higher than that in original herb, while the contents of other compounds in rat are quite lower than those in PRE, suggesting that

CKL might be the predominant existence form of APs.

4. Conclusions

The procedure proposed in current study was successfully applied to characterize the metabolite profile of PRE in rat. 10, 8 and 8 APs were unambiguously identified in plasma, urine and fecal samples of rat administrated by PRE with the assistance of reference compounds, respectively. In addition, another 21 (13 metabolites) APs in plasma, 10 (4 metabolites) APs in urine and 8 (4 metabolites) APs in feces were tentatively identified based on their mass spectra. Above all, MIM-IDA-EPI based on the prediction of metabolites (pMIM-IDA-EPI) provides a feasible option for characterization of tracing drug-related components in biological materials.

Acknowledgments

The research was supported by the National Basic Research Program of China 973 program (Grant No. 2009CB522707), the Macao Science and Technology Development Fund (077/2011/A3, 074/2012/A3) and the Research Fund of the University of Macau (MYRG 208 (Y3-L4)-ICMS11-WYT, and MRG012/WYT/2013/ICMS, MRG013/WYT/2013/ICMS).

References

1 E. Giovannucci, D.M. Harlan, M.C. Archer, R.M. Bergenstal, S.M. Gapstur, L.A. Habel, M. Pollak, J.G. Regensteiner and D. Yee, *CA-Cancer J. Clin.*, 2010, **60**, 207-221.

2 M.M. Gottesman, *Annu. Rev. Med.*, 2002, **53**, 615-627.

3 J.J. Monsuez, J.C. Charniot, N. Vignat and J.Y. Artigou, *Int. J. Cardiol.*, 2010, **144**, 3-15.

4 M.E. Franks, G.R. Macpherson, E.R. Lepper, W.D. Figg and A. Sparreboom, *Drug Resist. Update,* 2003, **6**, 301-312.

5 T. Xue and R. Roy, *Science*, 2003, **300**, 740-741.

6 C. Xiang, X. Qiao, Q. Wang, R. Li, W.J. Miao, D.A. Guo and M. Ye, *Drug Metab. Dispos.*, 2011, **39**, 1597-1608.

7 Z.X. Chen, B.S. Huang, Q.L. She and G.F. Zeng, *Yao Xue Xue Bao*, 1979, **14**, 486-496.

8 J.S. Ye, H.Q. Zhang and C.Q. Yuan, *Yao Xue Xue Bao*, 1982, **17**, 431-434.

9 National Commission of Chinese Pharmacopoeia (Eds.) Pharmacopoeia of the People′s Republic of China, vol. 1. Chemical Industry Press, Beijing, 2010, pp. 248.

10 H.M. Chang, P.P.H. But, S.C. Yao, L.L. Wang, S.C.S. Yeung, Pharmacology and Applications of Chinese Materia Medica; World Scientific Publisher: Singapore; 2001: (Vol 2) pp. 905.

11 I. Kostova, *Curr. HIV Res.*, 2006, **4**, 347-363.

12 X. Shen, G. Chen, G. Zhu, J. Cai, L. Wang, Y. Hu and W.F. Fong, *J. Pharm. Pharmaco.*, 2012, **64**, 90-100.

13 N.C. Zhao, W.B. Jin, X.H. Zhang, F.L. Guan, Y.B. Sun, H. Adachi and T. Okuyama, *Biol. Pharm. Bull.*, 1999, **22**, 984-987.

14 T.H. Chang, H. Adachi, T. Okuyama and K.Y. Zhang, *Acta Pharmacol. Sin.*, 1994, **15**, 388-391.

15 M. Yao, L. Ma, E. Duchoslav and M. Zhu, *Rapid Commun. Mass Spectrom.*, 2009, **23**, 1683-1693.

16 S. Ma and M. Zhu, *Chem. Biol. Interact.*, 2009, **179**, 25-37.

17 B. Wen and W. L. Fitch, *J. Mass Spectrom.*, 2009, **44**, 90-100.

18 M. Yao, L. Ma, W.G. Humphreys and M.S. Zhu, *J. Mass Spectrom.*, 2008, **43**, 1364-1375.

19 W. Yang, M. Ye, M. Liu, D.Z. Kong, R. Shi, X.W. Shi, K.R. Zhang, Q. Wang and L.T. Zhang, *J. Chromatogr. A*, 2010, **1217**, 4587-4600.

20 G. Hopfgartner, E. Varesio, V. Tschäppät, C. Grivet, E. Bourgogne, and L. A. Leuthold. *J. Mass Spectrom.*, 2004, **39**, 845-855.

21 D.R. Reyes, D. Iossifidis, P.A. Auroux and A. Manz, *Anal. Chem.*, 2002, **74**,

2623-2636.

22 Y.L. Song, W.H. Jing, R. Yan and Y.T. Wang, *J. Pharm. Biomed. Anal.*, 2014, **90**, 98-110.

23 Y. Song, H. Yan, J. Chen, Y. Wang, Y. Jiang and P.F. Tu, *J. Pharm. Biomed. Anal.*, 2014, **89**, 183-196.

24 Y. L. Song, W.H. Jing, G. Du, F.Q. Yang, R. Yan and Y.T. Wang, *J. Chromatogr. A*, 2014, **1338**, 24-37.

25 Y.L. Song, R. Yan, W.H. Jing, H.Y. Zhao and Y.T. Wang, *Rapid Commun. Mass Spectrom.* 2011, **25**, 719-730.

26 Y.L. Song, W.H. Jing, H.Y. Zhao, R. Yan, P.T. Li and Y.T. Wang, *Xenobiotica*, 2012, **42**, 231-247.

27 W.H. Jing, Y.L. Song, R. Yan, H.C. Bi, P.T. Li and Y.T. Wang, *Xenobiotica*, 2011, **41**, 71-81.

28 Y.L. Song, Q.W. Zhang, Y.P. Li, R. Yan and Y.T. Wang, *Molecules*, 2012, **17**, 4236-4251.

29 W.H. Jing, Y.L. Song, R. Yan and Y.T. Wang, *J. Pharm. Biomed. Anal.*, 2013, **77**, 175-188.

30 Y.L. Song, W.H. Jing, P.F. Tu and Y.T. Wang, *Nat. Prod. Res.*, 2014, **28**, 545-550.

31 Y.L. Song, W.H. Jing, F.Q. Yang, Z. Shi, M.C. Yao, R. Yan and Y.T. Wang, *J. Pharm. Biomed. Anal.*, 2014, **88**, 269-277.

32 M. Suzuki, Y. Li, P.C. Smith, J.A. Swenberg, D.E. Martin, S.L. Morris-Natschke and K.H. Lee, *Drug Metab. Dispos.*, 2005, **33**, 1588-1592.

33 X.M. Zhuang, J.T. Deng,H. Li, W.L. Kong, J.X. Ruan and L. Xie,Y*ao Xue Xu Bao*, 2011, **32**, 1276-1284.

34 X.M. Zhuang, Y.Y. Wen, H. Li, J.T. Deng, W.L. Kong, X.T. Tian, S.L. Cui and L. Xie, *Acta Pharmacol. Sin.*, 2010, **45**, 1116-1122.

35 A.E. Nassar and P.E. Adams, *Curr. Drug Metab.*, 2003, **4**, 259-271.

36 D. Lazewska, K. Kiec-Kononowicz, S. Elz, H.H. Pertz, H. Stark and W. Schunack, *Pharmazie*, 2005, **60**, 403-410.

37 H. Yusuor, W. Zou, V. V. Tolstikov, R. S. Tjeerdema and A. J. Fischer, *Plant Physiol.*, 2010, **153**, 319-326.

Figure Legends

Figure 1 Chemical structures of 11 reference compounds. CKL: *cis*-khellactone; CAK-4: *cis*-4′-angelylkhellactone; TAK-4: *trans*-4′-angelylkhellactone; TAK-3: *trans*-3′-angelylkhellactone; AAK: *cis*-3′-angeloyl-4′-acetylkhellactone; IAK: *cis*-3′-isovaleryl-4′-acetylkhellactone; PA: praeruptorin A; ASK: *cis*-3′-angeloyl-4′-senecioylkhellactone; PB: praeruptorin B; PE: praeruptorin E; DIK: *cis*-3′,4′-diisovalerylkhellactone.

Figure 2 Typical total ion current chromatograms of MRM scan. A was extract; B was plasma at 30 min; C was urine; D was feces. CKL: *cis*-khellactone; CAK-4: *cis*-4′-angelylkhellactone; TAK-4: *trans*-4′-angelylkhellactone; TAK-3: *trans*-3′-angelylkhellactone; AAK: *cis*-3′-angeloyl-4′-acetylkhellactone; PA: praeruptorin A; IAK: *cis*-3′-isovaleryl-4′-acetylkhellactone; ASK: *cis*-3′-angeloyl-4′-senecioylkhellactone; PB: praeruptorin B; PE: praeruptorin E; DIK: *cis*-3′,4′-diisovalerylkhellactone.

Figure 3 Proposed metabolic pathways of angular-type pyranocoumarins in rat.

Table 1 The retention time (t_R) and mass parameters of eleven reference pyranocoumarins in Peucedani Radix and APs identified by MRM from plasma, urine and feces samples of PRE group

Compound	t_R (min)	Ion pairs	DP (V)	CE (eV)	P	U	F
CKL	3.99	263>245	86	15	√	√	√
		263>203	86	21			
CAK-4	23.31	367>267	80	21	√	√	√
		367>245	80	33			
TAK-4	24.55	367>267	80	21	√	√	√
		367>245	80	33			
TAK-3	25.43	367>267	80	21	√	√	√
		327>227	77	23			
AAK	35.60	409>309	130	26	ND	ND	ND
		409>245	130	34			
PA	36.30	409>327	130	24	√	√	√
		409>227	130	30			
IAK	38.34	411>351	130	25	√	√	√
		411>245	130	35			
ASK	45.20	449>327	130	29	√	√	√
		449>227	130	44			
PB	46.91	449>327	130	29	√	√	√
		449>227	130	44			
PE	49.24	451>327	130	16	√	√	√
		451>227	130	32			
DIK	51.78	453>329	130	16	√	√	√
		453>245	130	40			

(P: plasma; U: urine; F: feces; ND: not detected; √: detected)

Table 2 Herb-related angular-type pyranocoumarins in plasma, urine and feces from the rats receiving an oral dosage of PRE using pMIM-IDA-EPI

MIM	Prediction	t_R (min)	Product ion	identification	P	U	F
245	hydrolysis	-	-	-	ND	ND	ND
247	prototype	-	-	-	ND	ND	ND
261	hydrolysis	4.80	243	3′-keto-3′,4′-dihydroseselin or 4′-keto-3′,4′-dihydroseselin	√	√	√
		5.74	243	3′-keto-3′,4′-dihydroseselin or 4′-keto-3′,4′-dihydroseselin	√	√	√
263	prototype	2.85	245, 203	compound **1**	√	√	√
		3.94	245, 203	CKL	√	√	√
285	prototype	-	-	-	ND	ND	ND
305	prototype	9.47	245, 227	compound **6**	√	√	ND
309	prototype	-	-	-	ND	ND	ND
327	prototype	9.48	227, 203	compound **6**	√	√	ND
341	hydrolysis	-	-	-	ND	ND	ND
355	hydrolysis	-	-	-	ND	ND	ND
357	hydrolysis+mono-oxidation	-	-	-	ND	ND	ND
365	prototype	30.75	261, 243	compound **22**	√	ND	ND
367	parent	23.43	267, 203	CAK-4	√	ND	ND
		24.55	267, 203	TAK-4	√	ND	ND
		25.43	227, 245, 203	TAK-3	√	√	√
371	hydrolysis+mono-o	-	-	-	ND	ND	ND

	xidation						
381	mono-oxidation	-	-	-	ND	ND	ND
383	mono-oxidation	17.37	267, 245, 227	mono-oxidation of compound **15**	√	ND	ND
385	mono-oxidation	12.10	267, 245, 203	mono-oxidation of compound **13**/**19**	√	ND	ND
		12.97	369, 327, 267, 245	mono-oxidation of compound **19**/**13**	√	ND	ND
393	prototype	-	-	-	ND	ND	ND
397	prototype	-	-	-	ND	ND	ND
399	di-oxidation	-	-	-	ND	ND	ND
401	di-oxidation	9.01	267	di-oxidation of compound **13**/**19**	√	ND	ND
409	prototype	36.30	349, 327, 227	PA	√	√	√
411	prototype	38.34	351, 329, 227	IAK	√	√	√
413	mono-oxidation	-	-	-	ND	ND	ND
423	prototype	-	-	-	ND	ND	ND
425	prototype	17.58	365, 227	compound **11**	√	√	√
		25.34	365, 227	mono-oxidation of PA	√	ND	ND
		26.15	365, 227	compound **17**	√	ND	ND
		31.36	365, 245	mono-oxidation of PA	ND	ND	√
		42.89	329, 245	compound **33**	ND	√	ND
427	mono-oxidation	18.37	367, 245, 227	mono-oxidation of IAK	√	ND	ND
		19.75	367, 245, 227	mono-oxidation of IAK	√	ND	ND
437	prototype/hydrolysis+glucuronidation	45.19	315, 245	compound **35**	ND	√	ND
439	prototype/glucuronidation	1.90	263, 203	glucuronidation of khellactone	ND	√	ND
441	di-oxidation	-	-	-	ND	ND	ND

443	prototype	11.27	383, 245, 227, 203	compound **8**	√	ND	√
		9.78	383, 245, 227, 203	compound **7**	ND	ND	√
447	oxidation	-	-	-	ND	ND	ND
449	prototype	45.23	349, 327, 227	ASK	√	√	√
		46.94	349, 327, 227	PB	√	√	√
451	prototype	49.28	349, 327, 227	PE	√	√	√
453	prototype	51.83	351, 329, 227	DIK	√	√	√
455	mono-oxidation	-	-	-	ND	ND	ND
457	di-oxidation	-	-	-	ND	ND	ND
461	glucuronidation	2.13	285, 263, 245	glucuronidation of khellactone	ND	√	√
465	mono-oxidation	38.23	365, 245, 227	mono-oxidation of PB	√	ND	ND
467	mono-oxidation	31.36	365, 245, 227	mono-oxidation of PE	√	ND	ND
469	mono-oxidation	-	-	-	ND	ND	ND
473	di-oxidation	-	-	-	ND	ND	ND
481	di-oxidation	-	-	-	ND	ND	ND
483	prototype	20.87	383, 245, 227	compound **12**	√	ND	ND
485	di-oxidation	19.78	367, 245, 227	di-oxidation of DIK	√	ND	ND
499	mono-oxidation	15.73	383, 245, 227	mono-oxidation of compound **12**	√	ND	ND
503	glucuronidation	-	-	-	ND	ND	ND
515	mono-oxidation	-	-	-	ND	ND	ND
543	glucuronidation	-	-	-	ND	ND	ND
545	glucuronidation	-	-	-	ND	ND	ND

(P: plasma; U: urine; F: feces; ND: not detected; √: detected)

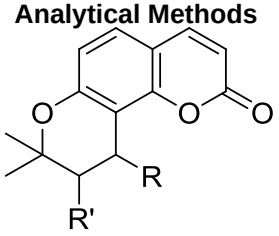

Compound	R′	R
CKL		
CAK-4		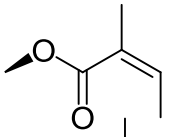
TAK-4		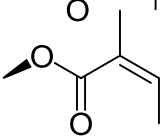
TAK-3	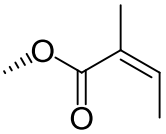	
AAK	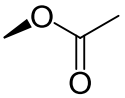	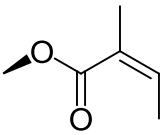
PA	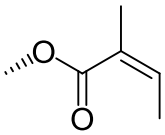	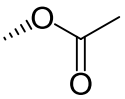
IAK	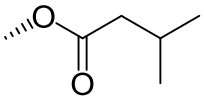	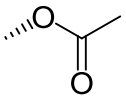
ASK	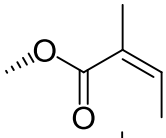	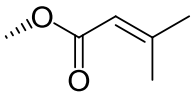
PB	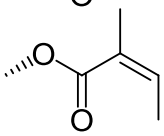	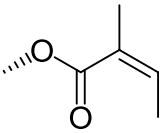
PE	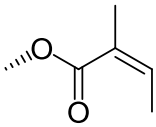	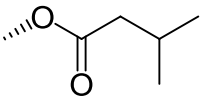
DIK	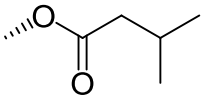	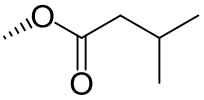

Figure 1 Chemical structures of 11 reference compounds. CKL: *cis*-khellactone; CAK-4: *cis*-4′-angelylkhellactone; TAK-4: *trans*-4′-angelylkhellactone; TAK-3: *trans*-3′-angelylkhellactone; AAK: *cis*-3′-angeloyl-4′-acetylkhellactone; IAK: *cis*-3′-isovaleryl-4′-acetylkhellactone; PA: praeruptorin A; ASK: *cis*-3′-angeloyl-4′-senecioylkhellactone; PB: praeruptorin B; PE: praeruptorin E; DIK: *cis*-3′,4′-diisovalerylkhellactone.

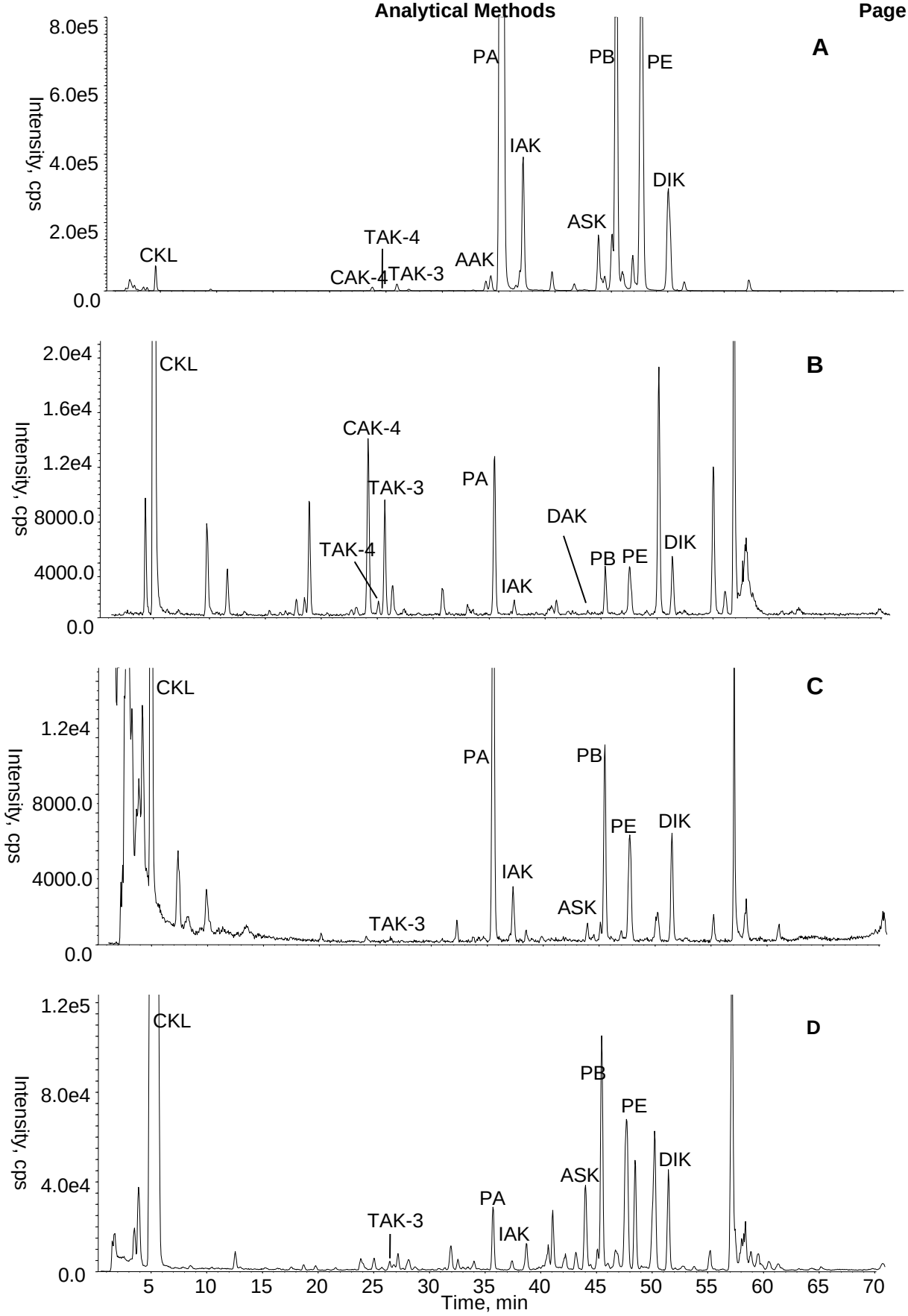

Figure 2 Typical total ion current chromatograms of MRM scan. A was extract; B was plasma at 30 min; C was urine; D was feces. CKL: *cis*-khellactone; CAK-4: *cis*-4′-angelylkhellactone; TAK-4: *trans*-4′-angelylkhellactone; TAK-3: *trans*-3′-angelylkhellactone; AAK: *cis*-3′-angeloyl-4′-acetylkhellactone; PA: praeruptorin A; IAK: *cis*-3′-isovaleryl-4′-acetylkhellactone; ASK: *cis*-3′-angeloyl-4′-senecioylkhellactone; PB: praeruptorin B; PE: praeruptorin E; DIK: *cis*-3′,4′-diisovalerylkhellactone.

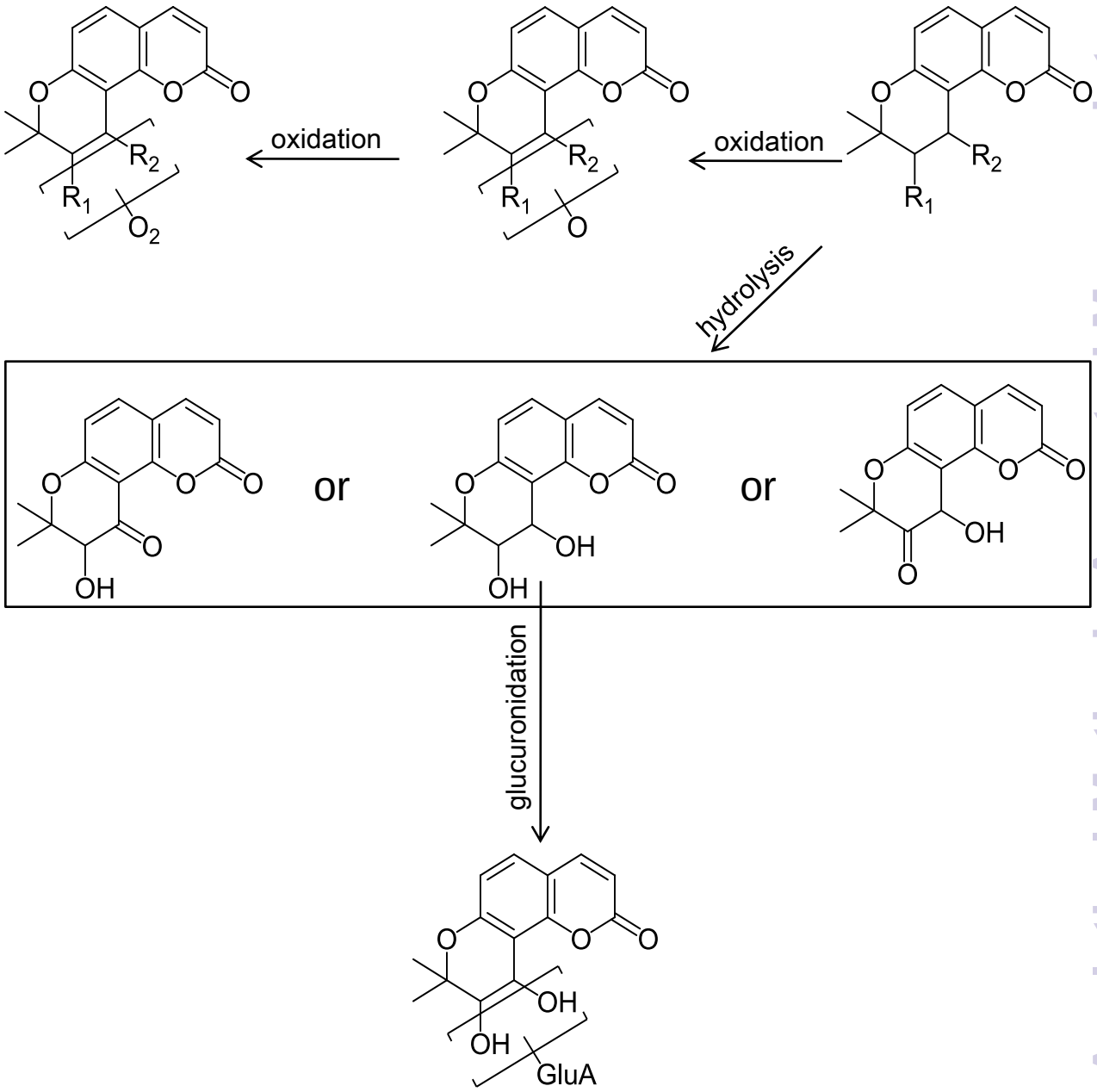

Figure 3 Proposed metabolic pathways of angular-type pyranocoumarins in rat.